Effect of freeze-thaw cycles on mechanical strength of lime-treated fine-grained soils

Thi Thanh Hang Nguyen, Yu-Jun Cui, Valéry Ferber, Gontran Herrier, Tamer Ozturk, Fabrice Plier, Daniel Puiatti, Simon Salager, Anh Minh A.M. Tang

Effect of freeze-thaw cycles on mechanical strength of lime-treated fine-grained soils

Thi Thanh Hang NGUYEN[1,2], Yu-Jun CUI[2], Valéry FERBER[3], Gontran HERRIER[1], Tamer OZTURK[1], Fabrice PLIER[4], Daniel PUIATTI[1], Simon SALAGER[5], Anh Minh TANG[2]

[1] *Lhoist R& D, Belgium*
[2] *Ecole des Ponts ParisTech, France*
[3] *Charier, France*
[4] *Urano, France*
[5] *Grenoble Alpes University, France*

Corresponding author

Dr. Anh Minh TANG

Ecole des Ponts ParisTech
6-8 avenue Blaise Pascal
77455 MARNE-LA-VALLEE
France

Email : anh-minh.tang@enpc.fr
Tel : +33 (0) 1 64 15 35 63
Fax : +33 (0) 1 64 15 35 62

Abstract

Lime treatment is a widely-used technique for the stabilization and improvement of fine-grained soils in earthworks for transportation. In cold regions, lime treatment can be considered as an appropriate method to improve freeze-thaw resistance of fine-grained soils. The effectiveness of treatment can depend on soil nature, lime dosage and curing time. In the present work, three soils (silt of low plasticity, clay of low plasticity, and silt of high plasticity) were treated at three lime contents (lower, equal and higher than the lime fixation point) at four curing periods (7, 28, 90 and 365 days). The mechanical strength was determined from unconfined compression test performed on specimens having a diameter of 100 mm and a height of 100 mm. Freeze-thaw cycles were applied by varying the specimen temperature between -20°C and 20 °C, the specimens being beforehand saturated. The mechanical strength of specimen subjected to ten freeze-thaw cycles was compared to those maintained in laboratory temperature (20 °C). Results showed that freeze-thaw cycles significantly decrease the mechanical strength of sample. This decrease can be explained by damage induced by ice lenses formation/thawing during freeze-thaw cycles, as illustrated by the observation at X-ray computed tomography. Interestingly, lime treatment mitigates this damage and increase the soil freeze-thaw resistance. The treatment appears more efficient for lower plasticity soil, a higher lime content, and a longer curing time. This conclusion seems depend on the specimen preparation procedure.

Key words: freeze-thaw cycles, lime content, fine-grained soils, ice lenses, curing time.

1. Introduction

Freeze-thaw (F-T) cycles related to seasonal change of temperature in cold regions can induce negative effects on the quality of road pavement. At the field scale, one of the main mechanisms inducing the degradation of the subgrade is the movement of water related to cryo-suction creating ice lenses in the frozen zone; thawing of these ice lenses significantly decreases the mechanical performance of the subgrade (Johnson et al., 1979; Benson & Othman, 1993; Shoop & Bigl, 1997; Zhang & Kushwaha, 1998; Zhang et al., 2014: Tang et al., 2018). At the material scale (i.e. microstructure level), F-T cycles create cracks, increase the hydraulic conductivity, and decrease the mechanical strength of fine-grained soils (Chamberlain & Gow, 1979; Graham & Au, 1985; Konrad, 1989a; Eigendbrod, 1996; Konrad & Samson, 2000; Qi et al., 2006). The creation of ice in soil pore, related to the movement of water due to cryo-suction, is also the main reason that induce soil structure modification and thus changes of soil properties (Konrad, 1989b). For a saturated sand/bentonite mixture, because of its low hydraulic conductivity that prevented the water movement, the effect of F-T cycles was not observed (Kraus et al., 1997; Podgorney & Bennett, 2006). In the case of unsaturated compacted fine-grained soils, F-T cycles also decrease the mechanical strength and stiffness (Lee et al., 1995; Wang et al., 2007; Qi et al., 2008; Ghazavi & Roustaie, 2010). Laboratory tests show that the F-T process, even without ice lenses formation, causes significant reduction in resilient modulus and unconfined compressive strength.

Lime treatment is usually used to improve the mechanical properties of fine-grained soils (Little, 1995; Prusinski & Bhattacharja, 1999; Parsons & Milburn, 2003; Al-Mukhtar et al., 2010; Tang et al., 2011; Wang et al., 2019). Actually, lime treatment of fine-grained soil creates cementitious compounds from pozzolanic reaction, coating the soil particles and

78 bonding them together (Al-Mukhtar et al., 2012; Tran et al., 2014; Wang et al., 2015; Ural,
79 2016; Wang et al., 2016; Wang et al., 2017). In addition, the improvement depends on both
80 lime content and curing time (Bell, 1996).
81
82 There have been a few studies dealing with the F-T resistance of lime treated fine-grained
83 soils. Liu et al. (2010) investigated the dynamic properties of a lime-treated clay soil
84 subjected to F-T cycles and found that lime treatment increased the durability of
85 stabilized soil under F-T cycles as compared to the unmodified samples. Hotineanu et al.
86 (2015) investigated the effect of F-T cycles on the mechanical properties of two types of
87 clayey soils, a high-plasticity bentonite and low-plasticity kaolinite. The results showed
88 that F-T cycles induced crack formation by the formation of ice lenses in the soil pores.
89 However, lime addition improved the strength of soil, either subject to F-T cycles or not.
90 Tebaldi et al. (2016) found that mechanical performances of a lime-stabilized clay soil was
91 less affected by F-T cycles compared to untreated soil. Bozbey et al. (2018) studied a lime
92 stabilized clay and found the importance of using higher lime contents and extended
93 curing time for increasing F-T resistance. In spite of the abovementioned works,
94 knowledge on the combined effects of curing time, lime content and soil's plasticity on the
95 F-T resistance of fine-grained soils is still limited and deserves to be further developed.
96
97 In this study, three soils, taken from three sites in France and in Belgium, having various
98 plasticity indexes were tested. For each soil, three lime contents (lower, slightly above,
99 and higher than the lime fixation point) were considered. Soil strength was determined
100 for various curing periods (7, 28, 90, and 365 days) with and without F-T cycles. The
101 results were finally discussed in the context of lime treatment for earthworks.
102

2. Materials

The properties of the soils used in this study are shown in Table 1 and the grain size distributions curves are shown in Figure 1. The clay fraction (< 2 micron) varies from 24% to 70% and the plasticity index varies from 7 to 34. Note that A1, A2 and A3 are the classification terms following the French standard (Afnor 1992). According to the Unified Soil Classification System (ASTM 2006), these soils are classified as silt of low plasticity, clay of low plasticity, and silt of high plasticity, respectively. In addition, these three types of soils are fine-grained soils that are usually used for earthworks. Soil A1 was taken from the excavation of a deposit of dolomite limestone in Marche-les-Dames (in Belgium); soil A2 was used for the construction project of the high-speed railway Tours-Bordeaux, France, and soil A3 was taken from a construction site in Charleville-Mézières, France.

Following X-ray diffraction results, soil A1 contains illite, kaolinite, chlorite, quartz, feldspath; soil A2 contains illite, kaolinite, chlorite, quartz, montmorillonite; and soil A3 contains illite, kaolinite, chlorite, montmorillonite, and quartz. X-ray fluorescence spectroscopy shows that the organic content of these soils is negligible.

The lime used is Proviacal ® ST, provided by the Lhoist company, which is a calcic quicklime (CaO) CL 90-Q (building lime), according to European Standard (CEN 2010), with an available CaO content of 90.1 %, and a t_{60} (reactivity) of 6.8 min.

In this study, each soil was treated with three different lime contents: (*i*) the minimum lime content, slightly lower than the lime fixation point (*LFP*), which corresponds to the short-term improvement objective; (*ii*) the intermediate lime content, slightly higher than the *LFP*; (*iii*) and the maximum lime content, higher than *LFP,* which corresponds also to the long-term stabilization objective. The *LFP* is the threshold lime content between the

improvement and stabilization objectives as lime added in excess of *LFP* can be mobilized for pozzolanic reaction. *LFP* is determined by soil – lime pH test following the protocol defined in ASTM (1999). LFP is the addition of lime needed for the maximum modification of soil, which gives an indication of the minimum quantity of lime that must be added to achieve a significant change in soil properties, mainly in terms of plasticity and compaction. The excess lime reacts with silicate tetrahedra and aluminate octahedra of the lattices of clay minerals (Al-Mukhtar et al. 2010). Thereby, the lime contents chosen are for soil A1 1%, 2% and 4%; for soil A2 1.5%, 3% and 5 % and for soil A3 2%, 4% and 7%.

The natural soil was firstly dried or humidified with water to reach the desired water content and then stored in a plastic box for 48 h for moisture homogenization. Then the moist soil and required lime content were mixed in a mixer for one hour prior to compaction.

Standard Proctor compaction and California Bearing Ratio (*CBR*) tests were first performed on specimens compacted by dynamic compaction in CBR mold of 150 mm high and 150 mm in diameter following ASTM (2005). The results on untreated and treated soils are presented in Figure 2. The compaction curves show that in comparison with the untreated soils, the treated soil has flatter compaction curves. In addition, at higher lime content, the optimum moisture content is higher and the maximum dry density is lower. The immediate bearing index (*IBI*) is generally improved with treatment. Note that for the soils of low plasticity, A1 and A2, the optimum can be easily detected from the compaction curves and the degree of saturation (S_r) at this state is close to 85%. By contrast, for soil A3 (high plasticity silt), the compaction curves are very flat; therefore, it

is difficult to determine the optimum moisture content. The optimum was then determined at the degree of saturation of 80 % following Afnor (1993a). The maximum dry density (ρ_{dmax}) and the optimum moisture content (w_{opt}) of natural and treated soils are shown in Table 2. Note that the water content of treated soils shown in this table was measured after the treatment. It can be observed that for all the three soils, at higher lime content the maximum dry density is lower and the optimum moisture content is higher. After Bell (1996), the reduction in maximum dry density could be due to an immediate formation of cementitious products which reduce compactibility and hence the density of the treated soil.

3. Experimental method

To assess the frost susceptibility of lime-treated soil in terms of damage induced by F-T cycles, tests were performed following the procedure suggested by CEN/TC 227/ WG4 (2010).

The soils were first treated with different lime contents and statically compacted (Afnor, 1993b) to obtain a dry density equal to 95% of the maximum Proctor dry density with a water content on the wet side of the Standard Proctor curve. The initial conditions of the tested specimens are shown in Table 2.

The dimensions of the compacted specimens are 100 mm in diameter and 100 mm in height. After the compaction, the specimen was covered with plastic film and wax to avoid moisture exchange during the curing period. Four curing periods were investigated: 7, 28, 90 and 365 days. For each lime content and each curing period, four identical specimens were prepared. At the end of the curing period, all the specimens were immersed in a

water bath during two days for saturation. Afterwards, two specimens were removed from the water bath, surface dried and tightly wrapped in plastic film (set A) while the two other specimens remained in the water bath (set B). The specimens of set A were then placed in a temperature-controlled climate chamber and subjected to ten F-T cycles, each cycle lasting 24 h. The temperatures measured at the center of the specimen and in the climate chamber during a preliminary test are plotted in Figure 3. The measures show that the soil temperature varied from 20 °C to -20 °C during this cycle.

After the completion of the F-T cycles, all the four specimens (in a saturated and surface dry condition) were subjected to unconfined compression test. The experimental device is shown in Figure 4. The axial force applied to the specimen (via a mechanical press) was increased by a constant rate of 150 N/s until failure. The strength of the sample was calculated as the ratio of the maximal force to the cross-section area of the sample. The retained strength factor (RFT), after F-T cycles, was then calculated as follows: $RFT = M_A/M_B$, where M_A and M_B are the average strengths of the sets A and B, respectively. As the set A was subjected to F-T cycles and the set B was not, RFT represents the frost susceptibility of the material. It is close to 1 when the soil's strength is not affected by the F-T cycles.

Besides, one sample subjected to F-T cycles was scanned with X-ray computed tomography (XRCT) in order to observe the cracks developed inside the specimen. The experimental setup of the XRCT scan is shown in Figure 5. The visualized parameter from XRCT observations was the linear attenuation coefficient, which was represented as a grey level. This parameter depended on density, the atomic number and the used X-ray energy (Molinero Guerra et al. 2018).

205

206 ## 4. Experimental results

207

208

209 The results obtained with soil A1 are shown in Figure 6. It appears that the strength of set
210 B (without F-T cycles) treated with a lime content of 1% (corresponding to the short-term
211 improvement objective) remained almost independent of the curing time (Figure 6a),
212 except the values at 90 days which were unusually high. Set A treated with a lime content
213 of 1% was heavily damaged by the F-T cycles and its strength is null for any curing time
214 (Figure 6b). As a result, the retained strength factor of soil A1 treated with a lime content
215 of 1% was null for any curing time (Figure 6c). Note that the results of all the specimens
216 (two specimens for each curing time) are shown in the Figures 6a and 6b (the lines show
217 the mean values) while only the mean values of retained strength factor are shown in the
218 Figure 6c.

219

220 In the case of soil A1 treated with a lime content of 2% and 4% (corresponding to the
221 long-term stabilization objective), the strength of set B (without F-T cycles) was higher at
222 a longer curing time (Figure 6a). RFT of the samples treated with 2% of lime content
223 remained negligible (lower than 20%) for short curing times (7 and 28 days); but it
224 reached 60-70 % for longer curing times (90 and 365 days) (Figure 6c). For sample
225 treated with 4% lime content, even at short curing times (7 and 28 days), the RFT already
226 reached 30%. At 365 days, it reached to 90%.

227

228 The results obtained on soil A2 are shown in Figure 7. As in the case of soil A1, Set B
229 treated with a small lime content corresponding to the short-term improvement objective
230 had a strength independent of the curing time, while the strength of set A (subjected to F-

T cycles) was almost null. In the case of soil specimens treated with a high lime content corresponding to the long-term improvement objective, the strength was higher at a higher curing time (Figure 7a). It is interesting to note that the strength of set B treated with 3% of lime content was equal to that with 5% of lime content up to 90 days. Only with 365 days of curing the strength of the specimens treated with 5% of lime content was twice higher than those treated with 3% of lime content. The influence of lime content on the strength of set A (subjected to F-T cycles) could be detected earlier (Figure 7b); the strength of the specimens treated with 5% lime content was similar to those of 3% in short curing times (7 and 28 days), but became 3-4 times higher at longer curing times (90 and 365 days). Finally, when analyzing RFT versus curing time (Figure 7c) for the specimens treated with 3% and 5% lime contents, the higher lime content had slightly higher RFT at 7 days but significantly higher RFT at longer curing times. In addition, RFT of soil A2 remained significantly lower (60%) than that of soil A1 (90%), even at long curing time.

The results obtained on soil A3 are presented in Figure 8. Again, the strength of set B treated with a lime content of 2% (corresponding to the short-term improvement objective) was found to be independent of curing time (Figure 8a). At higher lime content, higher strength could be observed only after 90 days of curing. It should be noted that lime treated with a lime content of 4% had a strength slightly higher than that at 7%. This could be explained by the fact that the dry density of specimens treated with a lime content of 7% (1.25 Mg/m^3) is significantly lower than that at 4% (1.31 Mg/m^3), see Table 2. After applying the F-T cycles, all the samples of set A were severely damaged and the strength are almost negligible (Figure 8b); M_A was null for soil with 2% and 4% of lime

content. Results on RFT show that even with higher lime content (7%) and long curing time (90 and 365 days), RFT reached only 20%. For the other cases, RFT was null.

In order to better understand the mechanisms related to the effect of F-T cycles on the strength of lime-treated soils, an X-ray computed tomography scan was performed on the sample within soil A1, treated with 2% of lime content, cured at 28 days, and subjected to 10 F-T cycles. The voxel size was 77 microns. The vertical slide (Figure 9a) shows that the soil was quite homogenous in the central zone. However, at the zones close to the borders, several cracks can be observed. In these zones, some soil aggregates could be also identified. In addition, close the side borders, vertical cracks were dominated while horizontal cracks could be clearly observed close to the top of the specimen. Figure 9b (horizontal slide in the middle of the specimen's height) and Figure 9c (horizontal slide at the bottom of the specimen) also show several cracks close to the border. In addition, the cracks created several concentric arcs.

Figure 10 shows images equally taken from soil A1, treated with 2% of lime content, cured at 28 days. It can be observed that the F-T cycles clearly created concentric arcs on the set A (Figure 10b) visible from the surface of the specimen while the surface of the set B remains intact (Figure 10a).

In order to assess the effect of number of F-T cycles on the results, *RFT* was determined at various F-T cycles for a series of soil specimens (soil A1, treated with 2% of lime content, cured at 28 days). The results are shown in Figure 11. It can be seen that RFT_N (retained strength factor at N cycles) reduced quickly from 100% to 55% only after the first cycle. It remained constant at 40% after 5 cycles. These results hence confirm that the choice of 10 cycles (mentioned in procedure suggested by CEN/TC 227/ WG4 (2010)) is appropriate to investigate the frost susceptibility of these soils.

5. Discussion

The results show that the kinetics of the variations of strength of lime-treated soils can be divided into two phases: the first one corresponds to a low increase of strength (up to 28 days of curing), and the second one corresponds to a significant increase of this parameter when the lime content is high. Actually, the first phase is usually explained by the immediate reactions of cation exchange and flocculation-agglomeration. After Little (1995), the soil improvement during this phase is reflected by the improved workability and immediate bearing capacity, as well as the increase of cohesion. In this study, the improvement of workability can be observed through the compaction curves (Figure 2) where immediate strength increase is identified from the results of IBI. Another evidence of this first phase is the fact that the soil strength measured at 7 and 28 days was independent of the lime content (Figures 6a, 7a, 8a). The second phase corresponds to the pozzolanic reactions that take longer time. After Al-Mukhtar et al. (2010), the excess of lime added promotes pozzolanic reactions and produces new minerals. Little (1999) stated that this phase can last 10 years under constant water content and temperature. Furthermore, the starting time of the second phase is different from one soil to another, varying from several hours to several days even weeks: 10 days after Locat et al. (1990), 14 days after Rogers et al. (2006), and 21 days after Wild et al. (1993). In the case of low lime content (slightly lower than the lime fixation point, corresponding to the short-term improvement objective), lime would be no longer available for the second phase. For this reason, the second was not observed.

Application of F-T cycles decreased the strength of all the samples - *RFT* is lower than 100% (Figures 6c, 7c, 8c). This decrease can be explained by the damage induced by F-T cycles. At the specimen scale, damages are represented by cracks observed in Figure 9

306 and Figure 10. The following mechanism can be suggested: while freezing is applied, the
307 temperature in the climate chamber is decreased progressively from 20 °C to -20 °C. That
308 induces a progressive decrease of temperature inside the specimen. When the
309 temperature at one point inside the specimen reaches a critical value (slightly lower than
310 0 °C) where pore water starts to be converted into ice, ice lenses will be formed because
311 of cryo-suction absorbing water from the surrounding zone having higher temperature.
312 These ice lenses, generally parallel to the soil surface, would then create cracks inside the
313 specimen. This mechanism would explain the concentric shape of the cracks observed in
314 Figure 9b and Figure 10b. Konrad (1989a,b) suggested similar physical processes to
315 explain the creation of ice lenses during F-T cycles in clayey silts.
316
317 The application of F-T cycles equally induces modification of soil microstructure at the
318 aggregates scale. Hohmann-Porebska (2002) observed aggregates of fabric created by ice
319 lensing and the aggregates remained generally stable even after thawing. After Svensson
320 & Hansen (2010), ice lensing absorbed water from the surrounding zone and induced
321 dehydration of clay particle in the unfrozen zone. Cracks and larger voids induced by F-T
322 cycles at the aggregates scale were observed by Liu et al. (2019) and Olgun (2013)
323 through scanning electron microscopy.
324
325 When comparing the *RFT* of different soils treated with lime content corresponding to the
326 long-term stabilization objective, the results show that the lime-treatment was more
327 efficient to improve the F-T resistance in long-term of lower plasticity soil (A1) than the
328 higher plasticity soil (A3). Hotineanu et al. (2015) found similar phenomenon when
329 testing lime-stabilized kaolinite and bentonite. Actually, the effect of F-T cycles at the
330 aggregates scale is similar to the wetting-drying process (Svensson & Hansen 2010).

Higher plasticity soils would be more sensitive to F-T cycles than lower plasticity soils because of damages induced at the aggregates scale (Khattab et al., 2007; Tang et al., 2011).

The low efficiency of lime treatment on soil A3 was observed on both mechanical properties and F-T resistance. That can be partly explained by the heterogeneity of lime distribution after the compaction of specimen. In addition, the preparation/mixing method used for this plastic soil induces large macro-pores between aggregates. The large size of aggregate can also limit the diffusion of lime inside the aggregates. To avoid such problems, lime treatment of plastic soil would be done in two steps: (*i*) a small quantity of lime is first added to the wet soil prior to first mixing to reduce the water content and the aggregates size; (*ii*) once the soil aggregates size get smaller and the water content is lower, the remaining part of lime is added prior to the second mixing in order to allow a better distribution (and diffusion) of lime.

Application of the results observed in the present work to the earthwork for transportation should consider various aspects. First, the conditions tested in the laboratory are generally more severe than the field conditions: (*i*) saturation of soil specimen enhances the effect of F-T cycles; (ii) the amplitude of temperature (from 20°C to -20°C) is also higher than the annual temperature cycles observed in various cold regions; (*iii*) in the laboratory, F-T cycles were applied to the specimen under free-swelling conditions (specimen can expand during freezing), while in the field F-T cycles are applied under in situ stress state (which would reduce expansion induced by freezing). Second, as the damage was observed in the zone close to the soil specimen

surface (Figure 9), the results on mechanical properties of the soil specimen would strongly depend on the specimen's dimensions.

6. Conclusion

The effect of ten F-T cycles on the mechanical strength of lime-treated fine-grained soils was investigated in the laboratory. For this purpose, three soils (low plasticity silt A1, low plasticity clay A2, and high plasticity silt A3) were treated with three lime contents (lower, equal, and higher than the lime fixation point *LFP*) and for four curing periods (7, 28, 90, and 365 days). The following conclusions can be drawn:

- The treatment with lime content equal to or higher than LFP increased significantly the mechanical properties of low plasticity fine-grained soils (A1 and A2), while the increase was less obvious for high plasticity silt (A3). For instance, the mechanical strength of soil A1 treated with 5% of lime content increased from 0.53 MPa (after 7 days of curing) to 3.10 MPa (after one year of curing), i.e. six times. However, for soil A3 treated with 7% of lime content, it increased from 0.36 MPa (after 7 days of curing) to 1.31 MPa (after one year of curing), i.e. four times.
- The increase of mechanical properties is more obvious at curing period longer than 28 days. Significant change can still be observed between 90 days and 365 days. This confirms the two phases usually mentioned in lime treatment of fine-grained soil: the short-term one corresponds to the immediate flocculation and workability improvement, whereas the long-term one corresponds to the initiation and development of pozzolanic reactions.
- The treatment with lime content equal to or higher than LFP increased significantly the F-T resistance of low plasticity fine-grained soils (A1 and A2), but

it is inefficient for high plasticity silt (A3). For instance, for soils A1 and A2 treated with lime content higher than LFP, RFT remained higher than 60% after 90 days and 365 days of curing. However, for soil A3, RFT was equal to 20% in the best cases.

The results obtained in the present work would be helpful for the design of earthwork for transportation using lime-treated fine-grained soils in cold regions.

7. References

Afnor. Classification of materials for use in the construction of embankments and capping layers of road infrastructures. Paris, France. NF P 11 – 300. 1992.

Afnor. Soils – Investigation and testing – Determination of the compaction characteristics of a soil – Standard Proctor test (600 kN.m/m3) – Modified Proctor tests (2700 kN.m/m3). Paris, France. NF P 94-093. 1993a.

Afnor. Essais relatifs aux chaussées – Préparation des matériaux traités aux liants hydrauliques ou non traités – Partie 3 : fabrication en laboratoire de mélange de graves ou de sable pour la confection d'éprouvettes. NF P98-230-2. 1993b.

Al-Mukhtar M, Lasledj A, Alcover JF. Behaviour and mineralogy changes in lime-treated expansive soil at 20°C. Applied Clay Science 2010; 50: 191 – 198.

Al-Mukhtar M, Khattab S, Alcover JF. Microstructure and geotechnical properties of lime-treated expansive clayey soil. Engineering Geology 2012; 139-140: 17–27.

ASTM. Standard Test Method for using pH to estimate the soil - lime proportion requirement for soil stabilization. West Conshohocken, United State. D6276-99a. 1999.

ASTM. Standard Test Method for CBR (California Bearing Ratio) of Laboratory-Compacted Soils. West Conshohocken, United State. D1883 – 07. 2005.

ASTM. Standard Practice for Classification of Soils for Engineering Purposes (Unified Soil Classification System). West Conshohocken, United State. D2487 – 06. 2006.

Bell FG. Lime stabilization of clay minerals and soils. Engineering Geology 1996; 42: 223–237.

Benson CH, Othman MA. Hydraulic conductivity of compacted clay frozen and thawed in situ. Journal of Geotechnical Engineering 1993; 119: 276-294.

Bozbey I, Kulibay Kelesoglu M, Demir B, Komut M, Comez S, Ozturk T, Mert A, Ocal K, Oztoprak S. Effects of soil pulverization level on resilient modulus and freeze and thaw resistance of a lime stabilized clay. Cold Regions Science and Technology 2018; 151: 323 – 334.

CEN. Building lime. Definitions, specifications and conformity criteria. Brussels, Belgium. EN 459 – 1. 2010.

CEN/TC 227/ WG4. Test for unbound and hydraulically bound mixtures – Determination of frost susceptibility: Resistance of freezing and thawing of hydraulically bound mixtures. TG 3/4 N32. 2010.

421 Chamberlain EJ, Gow AJ. Effect of freezing and thawing on the permeability and structure
422 of soils. Engineering Geology 1979; 13: 73 – 92.

423 Eigenbrod KD. Effects of cyclic freezing and thawing on volume changes and
424 permeabilities of soft fine-grained soils. Canadian Geotechnical Journal 1996; 33: 529 –
425 537.

426 Ghazavi M, Roustaie M. The influence of freeze-thaw cycles on the unconfined
427 compressive strength of fiber-reinforced clay. Cold Regions Science and Technology
428 2010; 61: 125 – 131.

429 Graham J, Au VCS. Effects of freeze-thaw and softening on a natural clay at low stresses.
430 Canadian Geotechnical Journal 1985; 22: 69 – 78.

431 Hohmann-Porebska M. Microfabric effects in frozen clays in relation to geotechnical
432 parameters. Applied Clay Science 2002; 21: 77 – 87.

433 Hotineanu A, Bouasker M, Aldaood A, Al-Mukhtar. Effect of freeze-thaw cycling on the
434 mechanical properties of lime-treated expansive clays. Cold Regions Science and
435 Technology 2015; 119: 151 – 157.

436 Johnson TC, Cole DM, Chamberlain EJ. Effect of freeze-thaw cycles on resilient properties
437 of fine-grained soils. Engineering Geology 1979; 13: 247 – 276.

438 Khattab SA, Al-Mukhtar M, Fleureau JM. Long-Term Stability Characteristics of a Lime-
439 Treated. Journal of Materials in Civil Engineering 2007; 19: 358–366.

440 Konrad JM. Effect of freeze-thaw cycles on the freezing characteristics of clayey silt at
441 various overconsolidation ratios. Canadian Geotechnical Journal 1989a; 26: 217 – 226.

442 Konrad JM. Physical processes during freeze-thaw cycles in clayey silts. Cold Regions
443 Science and Technology 1989b; 16: 291 – 303.

444 Konrad JM, Samson M. Hydraulic conductivity of kaolinite-silt mixtures subjected to
445 closed-system freezing and thaw consolidation. Canadian Geotechnical Journal 2000; 37:
446 857 – 869.

447 Kraus JF, Benson CH, Erickson AE, Chamberlain EJ. Freeze-thaw cycling and hydraulic
448 conductivity of bentonite barriers. Journal of Geotechnical and Geoenvironmental
449 Engineering 1997; 123: 229 – 238.

450 Lee W, Bohra NC, Altschaeffl AG, White TD. Resilient modulus of cohesive soils and the
451 effect of freeze-thaw. Canadian Geotechnical Journal 1995; 32: 559 – 568.

452 Little DN. Handbook for stabilization of pavement subgrades and base courses with lime.
453 Lime Association of Texas. 1995.

454 Little DN. Evaluation of structural properties of lime stabilized soils and aggregates.
455 Volume 1: Summary of findings. National Lime Association. 1999.

456 Liu J, Wang T, Tian Y. Experimental study of the dynamic properties of cement- and lime-
457 modified clay soils subjected to freeze-thaw cycles. Cold Regions Science and Technology
458 2010; 61: 29 – 33.

459 Liu Y, Wang Q, Liu S, ShangGuan Y, Fu H, Ma B, Chen H, Yuan X. Experimental investigation
460 of the geotechnical properties and microstructure of lime-stabilized saline soils under
461 freeze-thaw cycling. Cold Regions Science and Technology 2019; 161: 32 – 42.

462 Locat J, Bérubé MA, Choquette M. Laboratory investigations on the lime stabilization of
463 sensitive clays: shear strength development. Canadian Geotechnical Journal 1990; 27:
464 294–304.

465 Molinero Guerra A, Aimedieu P, Bornert M, Cui YJ, Tang AM, Sun Z, Mokni N, Delage P,
466 Bernier F. Analysis of the structural changes of a pellet/powder bentonite mixture upon
467 wetting by X-ray computed microtomography. Applied Clay Science 2018; 165: 164 – 169.

468 Olgun M. The effects and optimization of additives for expansive clays under freeze-thaw
469 conditions. Cold Regions Science and Technology 2013; 93: 36 -46.

470 Parsons R, Milburn J. Engineering Behavior of Stabilized Soils. Transportation Research
471 Record 2003; 1837: 20–29.

472 Podgorney RK, Bennett JE. Evaluating the long-term performance of geosynthetic clay
473 liners exposed to freeze-thaw. Journal of Geotechnical and Geoenvironmental
474 Engineering 2006; 132: 265 – 268.

475 Prusinski J, Bhattacharja S. Effectiveness of Portland Cement and Lime in Stabilizing Clay
476 Soils. Transportation Research Record 1999; 1652: 215–227.

477 Qi J, Vermeer PA, Cheng G. A review of the influence of freeze-thaw cycles on soil
478 geotechnical properties. Permafrost and periglacial processes 2006; 17: 245 – 252.

479 Qi J, Ma W, Song C. Influence of freeze-thaw on engineering properties of silty soil. Cold
480 Regions Science and Technology 2008; 53: 397 – 404.

481 Rogers CD, Boardman D I, Papadimitriou G. Stress Path Testing of Realistically Cured Lime
482 and Lime/Cement Stabilized Clay. Journal of Materials in Civil Engineering 2006; 18: 259–
483 266.

484 Shoop SA, Bigl SR. Moisture migration during freeze and thaw of unsaturated soils:
485 modeling and large-scale experiments. Cold Regions Science and Technology 1997; 25: 33
486 – 45.

487 Svensson PD, Hansen S. Freezing and thawing of montmorillonite – A time-resolved
488 synchrotron X-ray diffraction study. Applied Clay Science 2010; 49: 127 – 134.

489 Tang AM, Cui YJ, Vu MN. Effects of the maximum soil aggregates size and cyclic wetting–
490 drying on the stiffness of a lime-treated clayey soil. Géotechnique 2011; 61: 421–429.

491 Tang AM, Hughes PN, Dijkstra TA, Askarinejad A, Brencic M, Cui YJ, Diez JJ, Firgi T,
492 Gajewska B, Gentile F, Grossi G, Jommi C, Kehagia F, Koda E, ter Maat HW, Lenart S,
493 Lourenco S, Oliveira M, Osinski P, Springman SM, Stirling R, Toll DG, Van Beek V.
494 Atmosphere-vegetation-soil interactions in a climate change context; impact of changing
495 conditions on engineered transport infrastructure slopes in Europe. Quarterly Journal of
496 Engineering Geology and Hydrogeology 2018. (https://doi.org/10.1144/qjegh2017-
497 103).

498 Tebaldi G, Orazi M, Orazi US. Effect of freeze-thaw cycles on mechanical behavior of lime-
499 stabilized soil. Journal of Materials in Civil Engineering 2016; 28: 06016002.

500 Tran TD, Cui YJ, Tang AM, Audiguier M, Cojean R. Effects of lime treatment on the
501 microstructure and hydraulic conductivity of Hericourt clay. Journal of Rock Mechanics
502 and Geotechnical Engineering 2014; 6: 399 – 404.

503 Ural N. Effects of additives on the microstructure of clay. Road Materials and Pavement
504 Design 2016; 17: 104 – 119.

505 Wang D, Ma W, Niu Y, Chang X, Wen Z. Effects of cyclic freezing and thawing on mechanical
506 properties of Qinghai – Tibet clay. Cold Regions Science and Technology 2007; 48: 34 –
507 43.

508 Wang Y, Cui YJ, Tang AM, Tang CS, Benahmed N. Effects of aggregate size on water
509 retention capacity and microstructure of lime-treated silty soil. Géotechnique Letters
510 2015; 5: 269 – 274.

511 Wang Y, Cui YJ, Tang AM, Tang CS, Benahmed N. Changes in thermal conductivity, suction
512 and microstructure of a compacted lime-treated silty soil during curing. Engineering
513 Geology 2016; 202: 114 – 212.

514 Wang Y, Duc M, Cui YJ, Tang AM, Benahmed N, Sun WJ, Ye WM. Aggregate size effect on
515 the development of cementitious compounds in a lime-treated soil during curing. Applied
516 Clay Science 2017; 136: 58 – 66.

517 Wang Y, Cui YJ, Benahmed N, Tang AM, Duc M. Changes of small strain shear modulus and
518 suction for a lime-treated silt during curing. Géotechnique 2019; (doi:
519 10/1680/jgeot.18.t.018)

520 Wild S, Abdi MR, Leng-Ward G. Sulphate expansion of lime-stabilized kaolinite: II.
521 Reaction products and expansion. Clay Minerals 1993; 28: 569–583.

522 Zhang ZX, Kushwaha RL. Modeling soil freeze-thaw and ice effect on canal bank. Canadian
523 Geotechnical Journal 1998; 35: 655 – 665.

524 Zhang L, Ma W, Yang C, Yuan, C. Investigation of the pore water pressures of coarse-
525 grained sandy soil during open-system step-freezing and thawing tests. Engineering
526 Geology 2014; 181: 233 – 248.
527

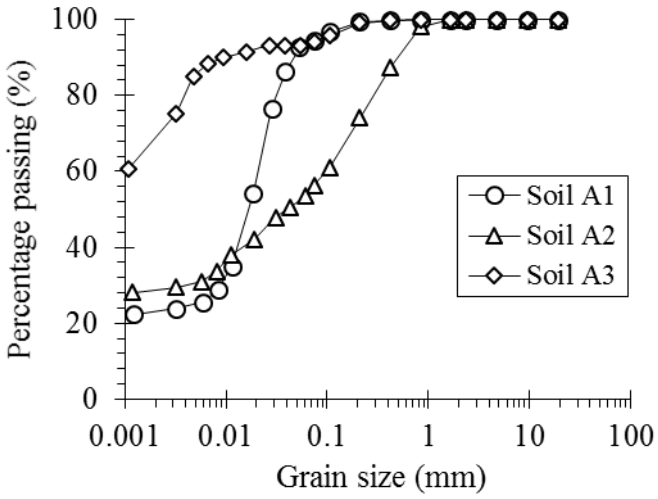

528
529 **Figure 1. Grain size distribution of the studied soils.**

530
531
532

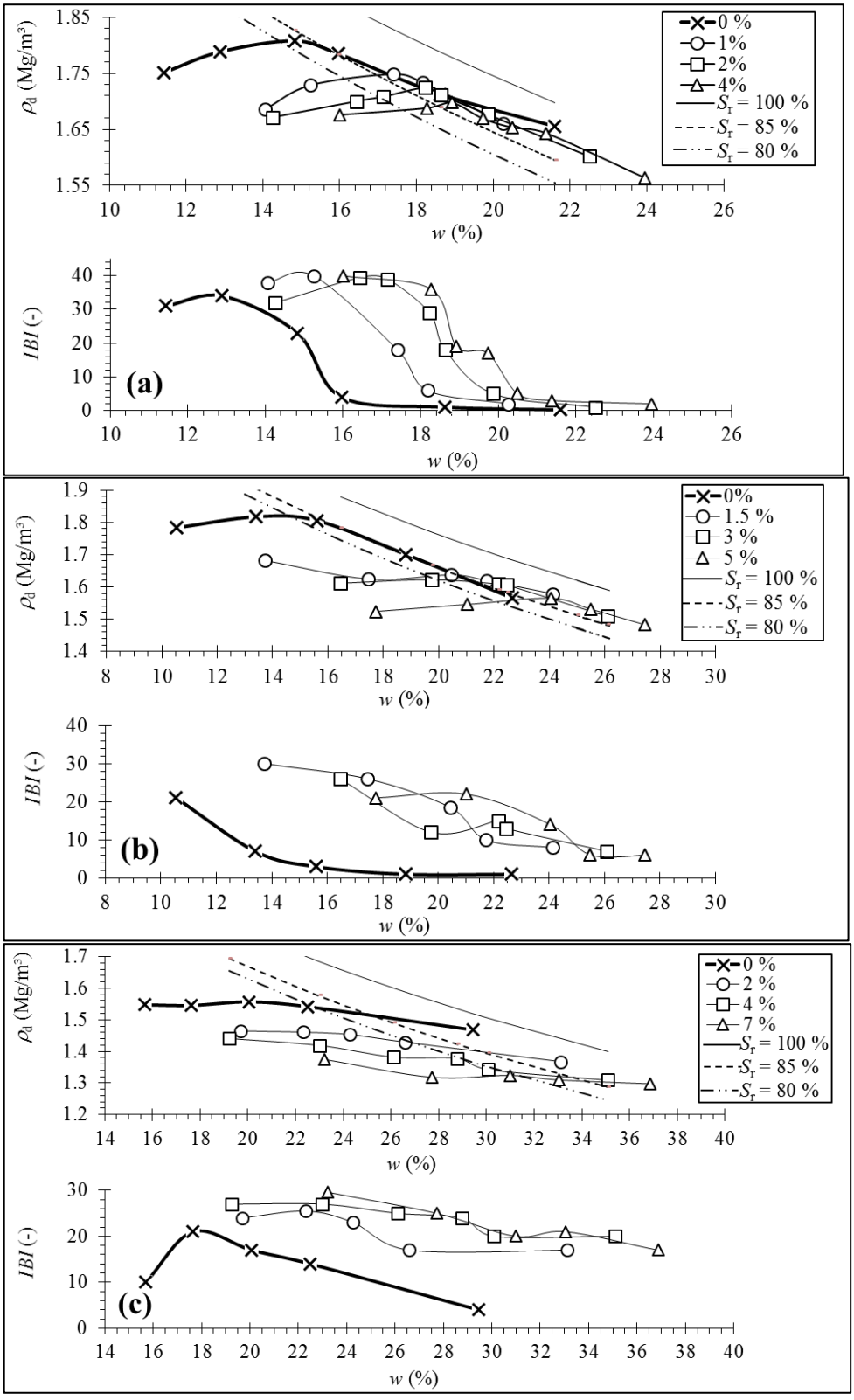

Figure 2. Results of Normal Proctor compaction and CBR tests: (a) soil A1; (b) soil A2; (c) soil A3.

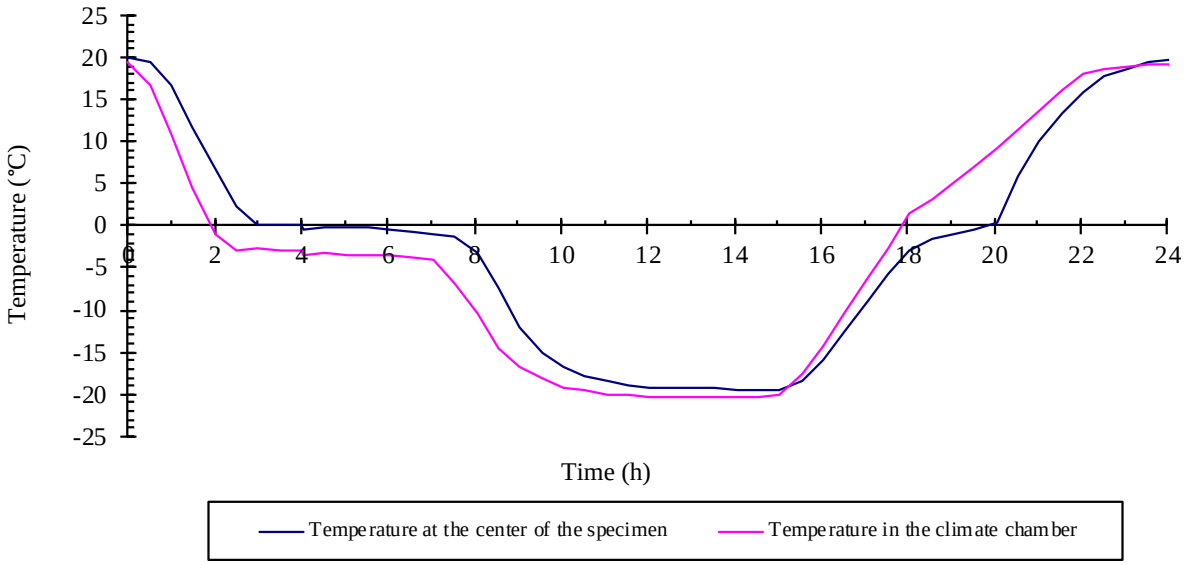

542
543
544
545 **Figure 3. Temperatures measured at the center of the specimen and in the chamber during a typical**
546 **freeze/thaw cycle.**

547

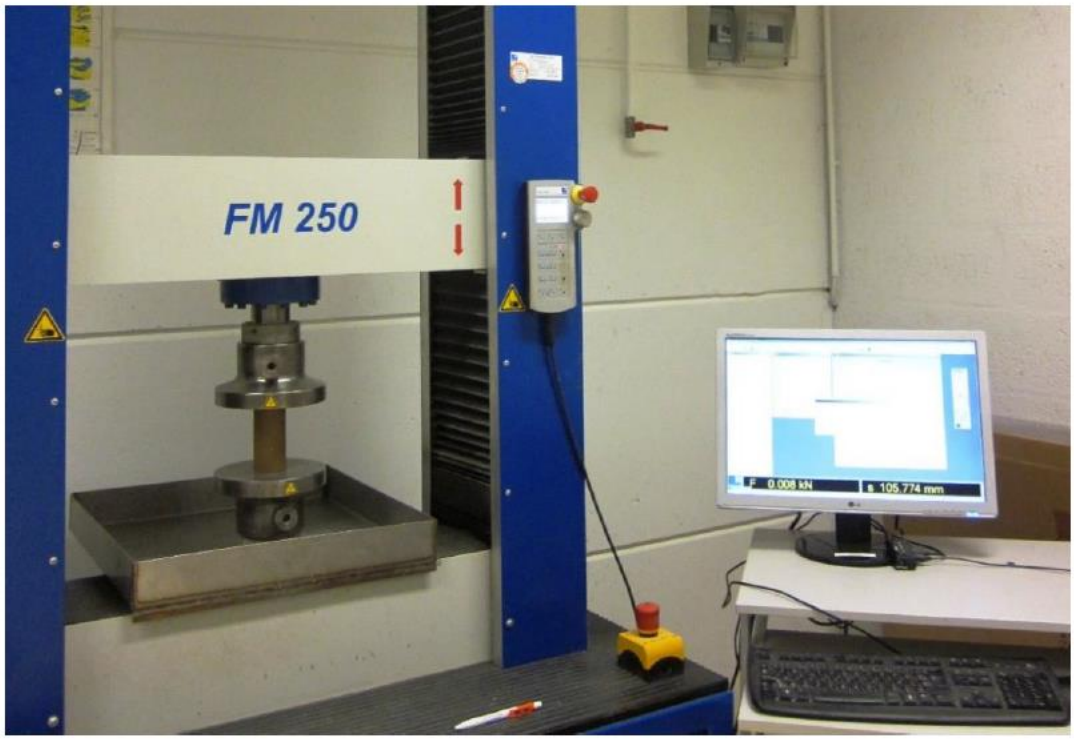

548
549 **Figure 4. Device to determine the mechanical strength.**

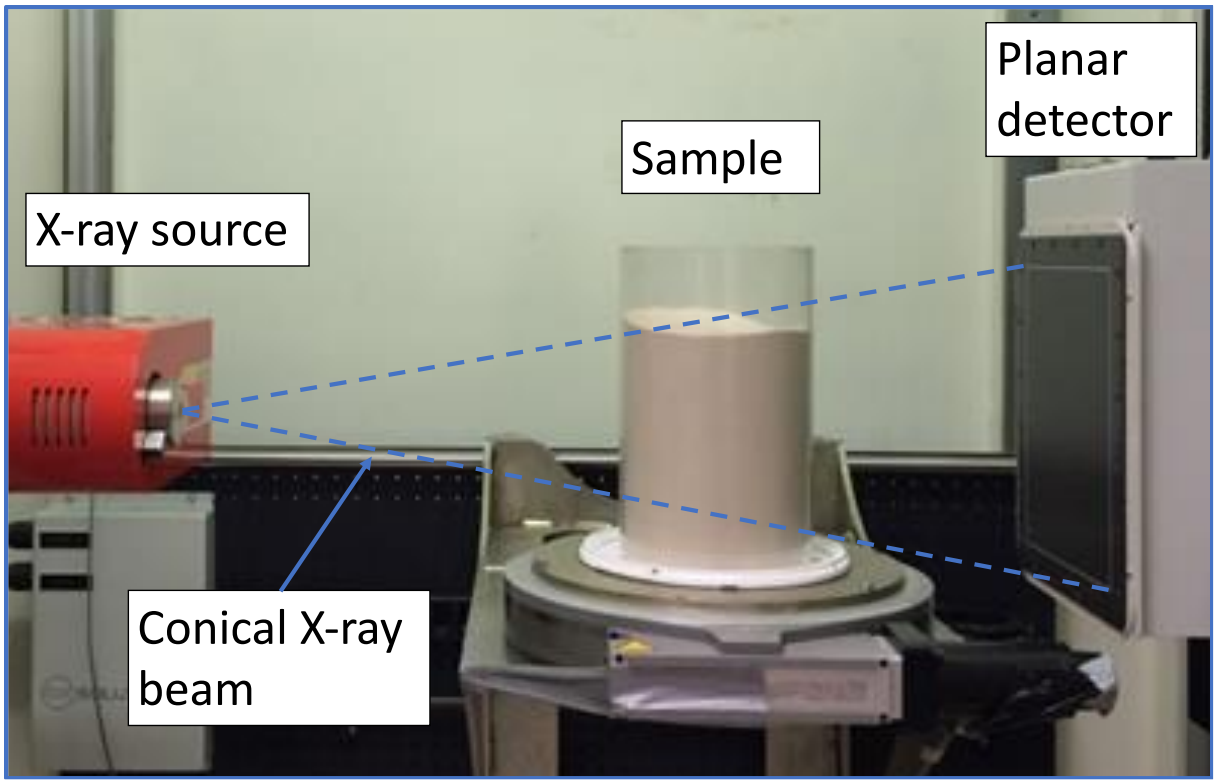

Figure 5. Device X-ray computed tomography.

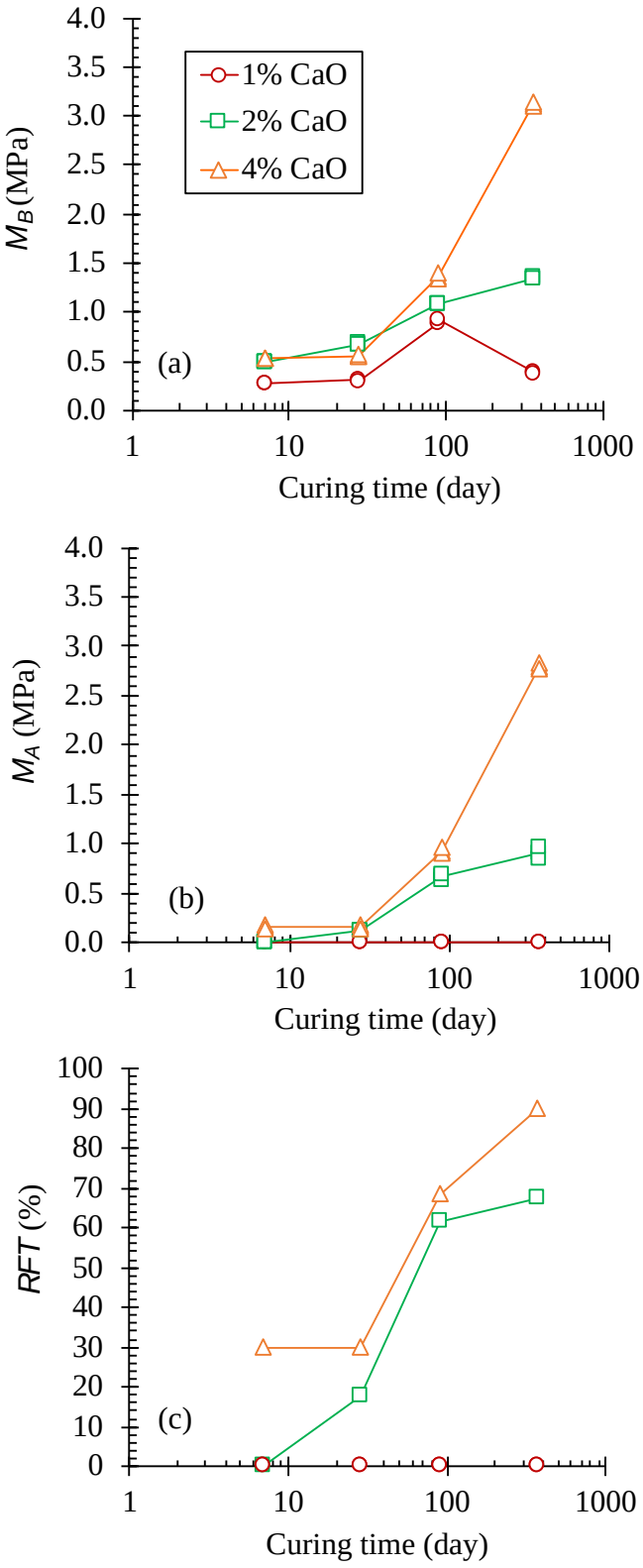

553

554 **Figure 6. Tests on soil A1: (a) strength of set B (without F-T cycles) versus curing time; (b) strength of set A**
555 **(with F-T cycles) versus curing time; (c) retrained strength factor versus curing time.**

556

557

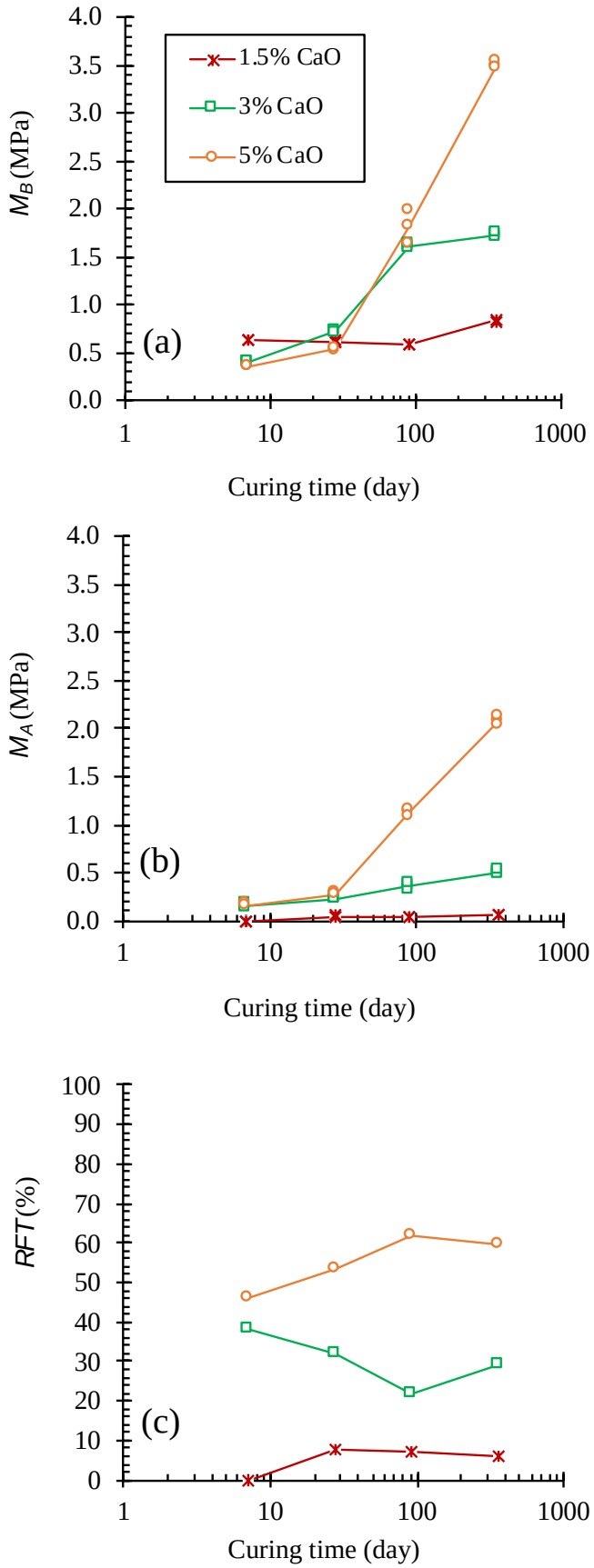

Figure 7. Tests on soil A2: (a) strength of set B (without F-T cycles) versus curing time; (b) strength of set A (with F-T cycles) versus curing time; (c) retrained strength factor versus curing time.

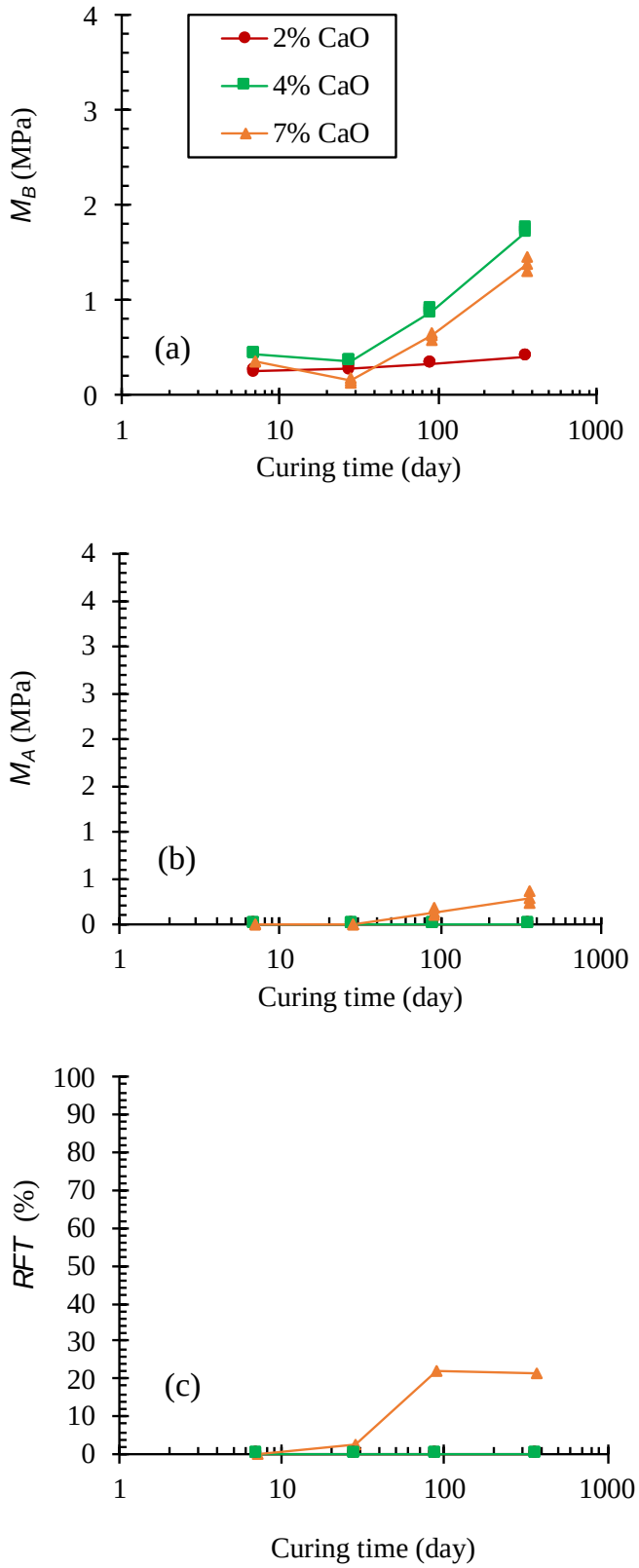

562
563 **Figure 8. Tests on soil A3: (a) strength of set B (without F-T cycles) versus curing time; (b) strength of set A**
564 **(with F-T cycles) versus curing time; (c) retrained strength factor versus curing time.**

565

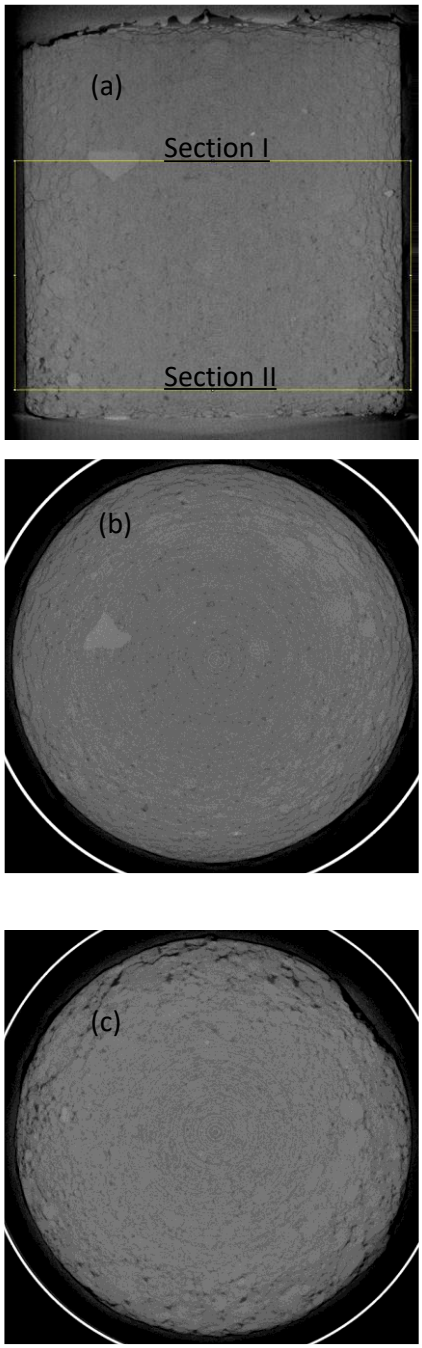

Figure 9. Image obtained by X-ray computed tomography on soil A1 treated with 2% of lime, at 28 days of curing under 10 F-T cycles: (a) vertical slide crossing the center of the sample; (b) horizontal slide in the middle of the sample – Section I; (c) horizontal slide at the bottom of the sample – Section II.

(a) (b)

Figure 10. Image obtained on soil A1 treated with 2% of lime, at 28 days of curing (a) Set B – without F-T cycles; (b) Set A – within F-T cycles.

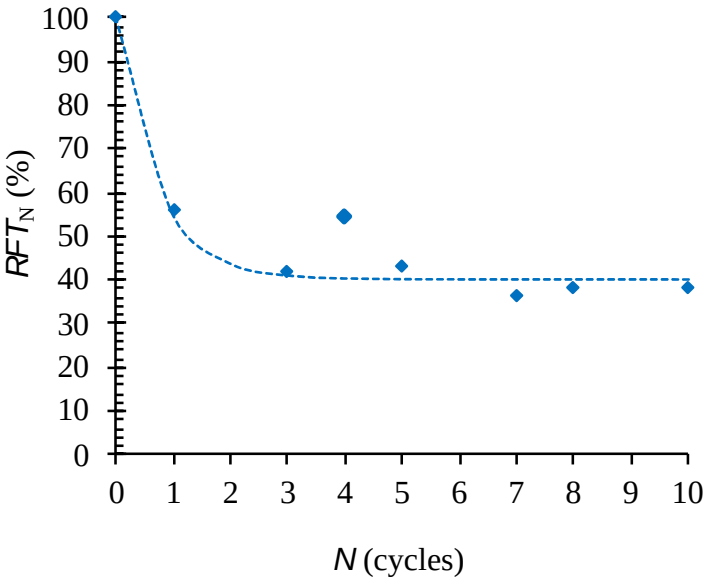

Figure 11. RFTN versus number of F-T cycles for soil A1 treated with 2% of lime, at 28 days of curing.

584
585 **Table 1. Properties of the soils studied**

586

Properties	Soil A1	Soil A2	Soil A3
Location	Marche-Les-Dames (Belgium)	Tours-Bordeaux (France)	Charleville-Mézières (France)
Fraction of size particle < 80 µm (%)	99	96	100
Fraction of size particle < 2 µm (%)	24	28	70
Methylene blue value, *MBV* (g/100g)	2.4	3.4	7.4
Plastic limit, w_P (%)	23.2	17.0	45.8
Liquid limit, w_L (%)	30.1	42.0	79.5
Plasticity index, *PI*	7	25	34
Classification (USCS)	ML	CL	MH

587
588
589
590
591
592
593
594
595
596
597
598
599
600
601
602

603 **Table 2. Optimum and Initial conditions of the tested specimens.**

		Optimum		Initial condition	
Soil	Lime content (%)	Maximum dry density (Mg/m^3)	Optimum water content (%)	Dry density (Mg/m^3)	Water content (%)
A1	0	1.81	14.8	-	-
A1	1	1.75	17.4	1.66	20.2
A1	2	1.72	18.2	1.63	21.4
A1	4	1.70	18.9	1.62	22.4
A2	0	1.81	15.6	-	-
A2	1.5	1.65	20.4	1.56	24.5
A2	3	1.61	22.2	1.54	25.5
A2	5	1.56	24.0	1.48	27.0
A3	0	1.56	20.1	-	-
A3	2	1.43	26.6	1.36	31.5
A3	4	1.38	28.8	1.31	35.1
A3	7	1.32	31.0	1.25	42.0

604

605